Published in final edited form as:
Gene Ther. 2008 October ; 15(19): 1330–1343. doi:10.1038/gt.2008.116.

Ex-vivo transduced autologous skin fibroblasts expressing human Lim Mineralization Protein-3 efficiently form new bone in animal models

Wanda Lattanzi[1], **Claudio Parrilla**[2], **Annarita Fetoni**[2], **Giandomenico Logroscino**[3], **Giuseppe Straface**[4], **Giovanni Pecorini**[4], **Egidio Stigliano**[5], **Anna Tampieri**[6], **Rossella Bedini**[7], **Raffaella Pecci**[7], **Fabrizio Michetti**[1,8], **Andrea Gambotto**[9], **Paul D. Robbins**[9], and **Enrico Pola**[3]

[1]Institute of Anatomy and Cell Biology, Università Cattolica del Sacro Cuore School of Medicine, Rome, Italy

[2]Department of Otolaryngology, Università Cattolica del Sacro Cuore School of Medicine, Rome, Italy

[3]Department of Orthopaedics, Università Cattolica del Sacro Cuore School of Medicine, Rome, Italy

[4]Department of Internal Medicine, Università Cattolica del Sacro Cuore School of Medicine, Rome, Italy

[5]Institute of Pathology, Università Cattolica del Sacro Cuore School of Medicine, Rome, Italy

[6]Institute of Science and Technology for Ceramics ISTEC-CNR National Council of Research, Faenza, Italy

[7]Technology and Health Department, Istituto Superiore di Sanità, Rome, Italy

[8]National Musculoskeletal Tissue Bank

[9]Department of Molecular Genetics and Biochemistry, University of Pittsburgh, School of Medicine, Pittsburgh, US

Abstract

Local gene transfer of the human LIM Mineralization Protein (LMP), a novel intracellular positive regulator of the osteoblast differentiation program, can induce efficient bone formation in rodents. In order to develop a clinically relevant gene therapy approach to facilitate bone healing, we have used primary dermal fibroblasts transduced *ex vivo* with Ad.LMP3 and seeded on an hydroxyapatite/collagen matrix prior to autologous implantation. Here we demonstrate that genetically modified autologous dermal fibroblasts expressing Ad.LMP-3 are able to induce ectopic bone formation following implantation of the matrix into the mouse triceps and paravertebral muscles. Moreover, implantation of the Ad.LMP-3-modified dermal fibroblasts into a rat mandibular bone critical size defect model results in efficient healing as determined by X-ray, histology and three dimensional micro computed tomography (3DμCT). These results demonstrate the effectiveness of the non-secreted intracellular osteogenic factor LMP-3, in inducing bone formation *in vivo*. Moreover, the utilization of autologous dermal fibroblasts

Correspondence should be addressed to E.P. (enrico.pola@rm.unicatt.it): Rome, Italy, Enrico Pola MD, PhD, Department of Orthopaedics, Università Cattolica del Sacro Cuore School of Medicine, Rome, Italy, enrico.pola@rm.unicatt.it, Fax: +39-0635500486, Tel: +39-0630154353.

Supplementary information is available at Gene Therapy's website.

implanted on a biomaterial represents a promising approach for possible future clinical applications aimed at inducing new bone formation.

Keywords

LMP; autologous transplantation; skin fibroblasts; gene therapy; bone formation; animal models

Introduction

Recombinant proteins, such as the bone morphogenetic proteins BMP-2 and BMP-7 (also known as osteogenic protein 1), have been used to enhance repair of non-union fractures and facilitate new bone formation in animal models as well as in clinical applications. However, a significant amount of recombinant BMP is required to promote osteogenesis and frequently the extent of new bone formation is low. In contrast, local gene transfer of BMPs has been shown to be more efficient in promoting osteogenesis in rodents than the use of recombinant proteins.[1] Several different types of gene transfer techniques have been utilized for inducing bone formation in animal models of bone defects.Direct injection of viral vectors, such as adenovirus, adeno-associated virus and lentivirus as well as implantation of plasmid DNA expressing BMPs or related osteogenic factors, have produced new bone in different models [2]. However, concerns about the immune response to the viral vectors and possible dissemination of the vectors have limited the clinical use of such approaches.

As an alternative to direct *in vivo* gene transfer, cell-based approaches, using cells genetically modified in culture to express an osteoinductive gene prior to implantation, have induced osteogenesis in different animal models. For the majority of these *ex vivo* approaches multipotent stem cells, isolated from mesenchymal-derived adult tissues (bone marrow stroma, muscle, adipose tissue, etc), expressing BMPs have been used successfully in different experimental models.[3–15] In addition, differentiated cell types also have been reported to be effective for delivery of BMPs to induce bone formation *in vivo.* [16–21]

BMP-2, 4, 8, 7 and 9 have all shown efficacy in facilitating bone formation in animal models. Similarly, gene transfer of intra-cellular proteins such as Osterix (OSX) and Lim Mineralization Protein (LMP) also have been shown to induce osteogenesis *in vivo*.[22, 23] In particular, LMP was first identified as a gene induced by steroids in secondary fetal rat calvarial osteoblasts that contained LIM domains in the carboxy terminal half of the protein.[24] The human LMP gene is alternatively spliced to produce three isoforms, LMP-1, -2 and -3, with LMP-1 being the most similar to the rat LMP. Human LMP-1 and LMP-3 have been shown to induce bone formation whereas LMP-2 does not exert osteogenic properties following gene transfer, but instead may inhibit osteogenesis.[25, 26] The mechanism through which LMP induces osteogenesis is still poorly defined, but appears to be mediated through the activation of genes involved in osteogenesis, including runt-related transcription factor 2 (RunX2), Osterix (OSX) and certain BMPs. Thus LMP seems to act as an upstream osteogenic factor. In addition, a region in LMP-1 and LMP-3 also has been demonstrated to interact with the Smad ubiquitination regulatory factor 1 (Smurf1), preventing ubiquitin-mediated degradation of the RunX2 and Smad proteins known to be involved in osteogenesis.[27]

We previously have demonstrated that adenoviral gene transfer of human LMP-3 (Ad.hLMP-3) facilitates ectopic bone formation following direct injection as efficiently as BMP-2.[28] However, concerns about the dissemination of the adenoviral vector have prevented the clinical application of Ad.LMP-3 for facilitating healing of critical size bone defects. Thus, in this study, we have developed a clinically relevant approach to induce bone

formation using autologous fibroblast isolated in primary culture from skin biopsies. Primary fibroblasts were transduced *ex vivo* to express LMP-3 and adsorbed on a novel nanocomposite osteo-conductive scaffold comprised of 20% hydroxyapatite and 80% collagen (HA/COL). We demonstrated that this cell-based treatment facilitates highly efficient ectopic bone formation in mice and healing of a mandibular bone defect in rats. The efficient induction of osteogenesis by LMP3-expressing fibroblasts clearly shows that intra-cellular LMP-3 is a potent osteoinductive agent. Moreover, given the limited invasiveness of the procedure for skin biopsy collection along with the easy isolation and *in vitro* expansion of dermal fibroblasts, this safe and effective approach could potentially lead to clinical applications.

Results

Ad-mediated transduction efficiency in dermal fibroblasts

Dermal fibroblasts were isolated in primary culture from skin biopsies obtained from each mouse and each rat employed in this study (animal models and surgical procedures are explained in the following paragraphs and in the methods section). Cells were expanded *in vitro* and then infected with defective adenoviral vectors carrying either the LMP-3 gene (Ad.LMP3) or the enhanced Green Fluorescent Protein (Ad.EGFP) gene. To determine if primary dermal fibroblasts could be efficiently transduced with adenoviral vectors, cells were infected with Ad.EGFP using an MOI of 100 plaque-forming units (pfu) per cell. EGFP-positive cells were then evaluated by fluorescence microscopy, which showed significant transgene expression at 24 hours (Figure 1a). The number of fluorescent cells approached 90% 48 hours post transduction (Figure 1b). Similar transduction efficiency, as measured by EGFP expression, was achieved in both murine- and rat-derived dermal fibroblasts (data not shown). In addition, cells were infected with Ad.LMP3 (100 MOI) and transgene expression evaluated at different time points by means of RT-PCR and quantitative real time PCR (qPCR), using sequence specific primers for the LMP gene. Both analyses were performed on multiple experiments using the RNA isolated from Ad.LMP3-transduced cells at different time points. Ad.EGFP-transduced cells served as controls. Both RT- and real time-PCR showed efficient LMP-3 expression 24 and 48 hours after infection with Ad.LMP3 (Figure 1c). Moreover quantitative real time PCR indicated that the transgene expression in transduced cells slightly increased in a time dependent manner up to 4 days post infection and then remain stable up to 14 days (Figure 1d).

Matrix mineralization *in vitro*

We have previously demonstrated that LMP3 transduction induces bone mineralization *in vitro* in both fibroblasts and osteoblasts cell lines [28]. Also dermal fibroblasts could not mineralize under basal conditions, but have the intrinsic potential to undergo mineralization upon an efficient osteogenic stimulus. In order to assess the *in vitro* osteogenic potential of engineered dermal fibroblasts prior to *in vivo* implantation, we evaluated the formation of a mineralized matrix in Ad.LMP-3-transduced cells by Alizarin staining, using EGFP-transduced cells as a negative control. *In vitro* mineralization could be observed as early as one week post Ad.LMP3-transduction, whereas no modification was observed in control cells (Figure 2a–b). Similar results were obtained in three independent replicate experiments (see supplemental file 1).

Delivery of engineered dermal fibroblasts using an osteo-conductive scaffold *in vivo*

To evaluate whether transduction of the dermal fibroblasts with Ad.LMP-3 could result in *in vivo* bone formation, autologous dermal fibroblasts were isolated from each animal (mice and rats) and independently transduced *ex vivo* with Ad.LMP3 prior to autologous implantation (animal models and surgical procedures are explained in the following

paragraphsand in methods). Thus autologous cells were used for implantation in recipient animals in order to mimic the clinical setting. To facilitate the delivery of cells, a nanocomposite osteo-conductive scaffold comprised of 20% hydroxyapatite and 80% collagen (HA/COL) scaffold was prepared and seeded with Ad.LMP3-transduced fibroblasts. Untransduced dermal fibroblasts seeded on the HA/COL scaffold and the unseeded scaffold were used as alternative negative controls.

Efficient cell colonization of the HA/COL matrix

In order to assess the effective colonization of the scaffold by functional cells (i.e. transduced cells expressing the transgene) mouse and rat dermal fibroblasts were transduced *ex vivo* with Ad.EGFP. The Ad.EGFP-transduced fibroblasts were then implanted in two recipient animals per exeperimental group (see following surgical procedures for details). Unseeded scaffolds were implanted in negative control animals. All animals were sacrificed one month after surgery and fresh tissue sections were analyzed for EGFP expression using an invertoscope equipped with a fluorescence-emitting lamp. Fluorescent cells were clearly detected in the nanocomposite structure in treated animals, while no morphological evidence of fluorescence cell was detected in control animals one month following the surgical procedure, demonstrating the successful colonization of the scaffold by the genetically-modified cells and their persistence over time (Figure 2c,d).

Ad.LMP-3 promotes efficient bone formation *in vivo*

The HA/COL scaffold seeded with engineered autologous dermal fibroblasts was implanted in recipient animals, in order to evaluate the *in vivo* osteogenic potential of the LMP3-cell construct. Naked scaffold and scaffold seeded with wild type cells served as controls. For this purpose we utilized three different experimental models: ectopic bone formation in mouse triceps and paravertebral muscles, along with a rat model of stable mandibular bone defect. The occurrence of bone formation at the site of implantation was then evaluated in time course by means of X-rays, histological analysis and micro computerized tomography (μCT), with 3D reconstruction. None of the animals displayed evidence of systemic or local toxicity related to either the implantation procedure or the *ex vivo* gene delivery technique.

Ectopic bone models

Initially the scaffold with seeded cells was inserted into mouse muscles, either into the triceps or the paravertebral muscle. The mice were then monitored for ectopic bone formation by X-ray and histology. In the group of mice receiving triceps implantation of the scaffold containing LMP3-transduced cells, 1/5 mice were positive by x-rays and histology at 2 weeks. After 1 month, 6/10 mice were positive by x-ray and histology, while 3/5 were positive by both assays after 2 months (Figure 3; Table 1). Control animals, treated with either EGFP-positive cells, non-transduced cells or unseeded scaffold (HA/COL nanocomposite with sterile PBS), were negative for bone formation at each time point tested. No significant differences among the control groups were detected (data not shown). Mice subjected to paravertebral implantation were positive for bone formation after 1 and 2 months as determined by X-ray and histology while the controls were negative for bone formation at both time points (Figure 4, Table 1). Moreover, all animals subjected to paravertebral implantation were examined also by 3DμCT, which showed a large dense mass in the site of implantation (figure 5c, d, f, g). This bone-like structure showed the same density of the vertebral bone as confirmed in the 3D reconstruction of the new formed mass (figure 5i, j) and in the cross sections, showing spots of cortical-like density (figure 5j). The mean volume (mean of volume values obtained from each treated animal) of the new formed bone, calculated by measuring the diameters of the mass in different cross sections for each animal, was 100 +/−7 mm^3 (see supplemental files 2, 3 and 4). In order to assess and quantify the structural features of the new formed mass, the following morphometric indexes

were calculated and compared for the whole mass and corresponding vertebral bone sections of same animals, following the procedures described by Muller and colleagues [29]: Tissue Volume (TV, mm3) = the total volume of interest (the whole new-formed mass and the vertebral body section respectively); Bone Volume (BV, mm3)= the sum of all voxels marked as bone inside the volume of interest; Bone Volume Fraction (BV/TV, %)= the ratio between BV and TV in percentage; Bone Thickness (BT, mm)= mean thickness of bone trabeculae within the bone volume, derived from bone volume and bone surface density; Degree of Anisotropy (DA)= corresponding to the preferential orientation(s) of trabeculae within the bone tissue Based on these calculations, the new formed bone displayed similar characteristics to the vertebral bone (Table 2). The 3DμCT analyses performed in control animals treated with either EGFP-positive cells, non-transduced cells or unseeded HA/COL resulted negative as no bone-like structure was evidenced at the site of implantation at each time point tested (figure 5a, b, e). In particular, no bone-like structure could be observed as earlier as 1 month after surgery in animals subjected to unseeded scaffold implant (see supplemental file 5). This result demonstrates that the naked osteo-conductive scaffold doesn not have an osteogenic effect. Taken together, these results demonstrate that Ad.LMP-3 transduction of autologous dermal fibroblasts followed by implantation on a HA/COL scaffold results in efficient bone formation in two different ectopic bone formation models.

Rat mandibular bone defect

To determine if the proposed *ex vivo* approach can be considered a potential therapeutic tool in a relevant animal model of bone formation, a rat mandibular bone defect was utilized. In this model, a 5 × 5 mm full-thickness defect was created in the exposed mandible behind the root of the incisor without interrupting the bone continuity (Figure 6a). The defect was filled with the scaffold seeded with either LMP3-transduced (group 1) or control cells (group 2) or with naked scaffold (group 3). Four animals per group were sacrificed at 4, 8 and 12 weeks, respectively, after surgical procedures for analysis of new bone formation by X-rays, histology and 3DμCT following sacrifice. In all the animals the entire regenerated mandible remained in its original position, without any sign of dislocation. All rats treated with autologous dermal fibroblasts transduced with Ad-LMP3 showed positive X-ray and histology at 8 and 12 weeks post-surgery, whereas only 1 out of 4 treated animals was positive as early as 4 weeks post surgery (Figure 6c, d, f, h, j). No evidence of bone formation could be demonstrated in 3/4 animals at the earliest time point (4 weeks) and in animals treated with scaffold alone or with non-transduced cells (Figure 6, b, e, g, i, k). Also, there were no significant differences observed among animals treated with either scaffold without cells or non-transduced fibroblasts at all time points (data not shown). The 3DμCT imaging studies revealed the successful repair of the defects implanted with LMP-3-cell constructs which occurred in a time-related manner until 12 weeks after implantation (figure 7b–d). Conversely, no bone formation was observed in the control group (figure 7a). The new bone surface area was calculated in each treated animal based on the measure of the mean diameter of the newly formed bone obtained from the CT lateral view of the rat skull (figure 7e–h). The mean area of the newly formed bone in the rat mandible was 100 +/− 4 mm^2 (mean of surface area values obtained from each animal plus standard deviation). The mean area of the original bone defect was 133 +/− 2 mm^2, indicating that 75% of the hole produced in the mandible was filled with newly mineralized tissue 12 weeks post surgery.

Discussion

Existing techniques employing gene transfer for the delivery of osteogenic factors such as BMPs and LMPs have raised concerns about the inability to target the preferred site for

induction of osteogenesis for *in vivo* applications. Thus we have focused our efforts on developing a clinically relevant gene therapy approach, based on the use of autologous implantation of primary dermal fibroblasts for facilitating targeted bone formation in different types of animal models. The data here obtained from *in vitro* experiments, prior to autologous cell implantation, confirmed that dermal fibroblasts, easily and rapidly isolated in primary culture, can be efficiently transduced with adenoviral vectors. It has been recently demonstrated the unsuspected potential plasticity of dermal fibroblasts, which could switch from a somatic differentiated phenotype to multipotency upon selected stimulations [30]. We have demonstrated that skin fibroblasts, which do not form bone under basal conditions, could undergo mineralization in vitro upon LMP-3-transduction, suggesting their intrinsic osteogenic potential, which could probably be effective in vivo after the implantation in recipient animals. However, we cannot exclude a role of other resident cells types, such as mesenchymal progenitors, in the osteogenic process induced by factors released by the transduced fibroblasts using the ex vivo procedure. Furthermore, these results indicated the effectiveness of the non-secreted, intracellular osteogenic factor, LMP-3, in inducing bone formation following delivery to autologous primary dermal fibroblasts in mice and rats. Specifically, the genetically modified autologous dermal fibroblasts were seeded on a biomaterial comprised of hydroxiapatite and collagen prior to implantation in order to target the site of desired new bone formation. We have previously demonstrated the exclusive bio-conductive and resorption properties of the HA-based scaffolds, which were unable to form bone following naked implantation (unseeded biomaterial) *in vivo* and resulted in negative X-rays [31]. Here we have demonstrated that transduction of the dermal fibroblasts with Ad.LMP-3 resulted in ectopic bone formation following implantation of the seeded scaffold into the mouse triceps and paravertebral muscles. Moreover, the implantation of the scaffold seeded with Ad.LMP-3-modified dermal fibroblasts into a rat mandibular bone critical size defect model resulted in efficient healing. The rat mandibular fracture used in this study represent a clinically relevant model as the defect is inherently stable over time, not being able to repair autonomously. In addition, for all the animal models employed, autologous dermal fibroblasts were isolated from each animal to be treated in order to more accurately reflect the clinical setting. These results thus demonstrated that dermal fibroblasts, easily and rapidly isolated in primary culture, can be efficiently transduced with adenoviral vectors.

It has been demonstrated by others that BMP-transduced cells can induce bone *in vivo*. In particular, efficient ectopic bone formation and healing of bone defects was achieved following the implantation of skin fibroblasts expressing BMP-2 and BMP-7.[18–21] However, in these *ex vivo* models, the osteoinductive potential seemed not to be related to the cell type, as BMPs are secreted and act as osteogenic molecules at the site of implantation. The type of vector used for gene delivery is more likely crucial to provide the correct level of transgenic protein for efficient osteoinduction.[19]

The advantage to use LMP as the osteogenic agent is that it is a non-secreted protein, unlike BMP-2, thus reducing any possible adverse effects due to high expression levels of an exogenous osteogenic factor. It has been demonstrated that LMP-3 osteoinductive properties are, at least in part, mediated through the up-regulation of the BMP2 gene [28,32,33]. Thus the cell delivery of LMP-3 could possibly supply more physiologic levels of osteogenic molecules produced *in vivo* by genetically modified cells. Also, gene transfer offers certain advantages over the use of recombinant proteins such as BMP-2 and BMP-7. The main limitation of using recombinant proteins for inducing bone formation in clinical applications is the need for delivery systems that provide a sustained, biologically appropriate concentration of the osteogenic factor at the site of the defect. Delivery needs to be sustained, because these factors have exceedingly short biological half-lives, usually of the order of minutes or hours, rather than the days or weeks needed to stimulate a complete

osteogenic response. Delivery also needs to be local in order to avoid ectopic ossification and other unwanted side effects. The use of local gene transfer offers great potential as a delivery system for osteogenic factors in that it meets the above requirements. Moreover, unlike recombinant protein, the growth factor synthesized *in situ* as a result of cell-based gene transfer undergoes authentic post-translational processing and is presented to the surrounding tissues in a natural, cell-based manner. In fact it has been reported that BMP-2 gene therapy produces a better response than recombinant BMP-2 protein in healing osseous defects in rats, although both approaches lead to osseous union.[1] The protocol described in this report represents a clinically relevant approach for facilitating new bone formation as it is based on the use of autologous cells, which can be obtained from a extremely small skin biopsy and easily cultured. Although adenoviral vectors are far from being adequate for gene therapy in the clinical setting, mainly due to the immune response, the use Ad.LMP-3 vector here provided a proof of the effectiveness of *ex vivo* gene delivery in this model. Alternative approaches to gene transfer, including the use of recombinant LMP-protein transduction domain fusion proteins and LMP derived peptides, are currently being tested and hopefully will lead to future potential therapeutic applications.

The molecular mechanisms involved in LMP-induced osteogenesis are still unclear. LMP has been shown to induce the expression of BMPs, RunX2, OSX, bone sialoprotein, osteocalcin, osteopontin and alkaline phosphatase, although it is not clear whether its role in transcription modulation is direct or indirect. [28,32,33] A region of LMP has been shown to bind to and inhibit the activity of Smurf1, increasing the levels of RunX2 and Smad proteins.[27] However, there are additional regions of LMP-1 and LMP-3 that are involved in osteogenesis. In fact, there appears to be at least three distinct regions in LMP-1 and LMP-3 able to induce the OSX promoter (unpublished observations), but the pathways targeted by these regions have not yet been elucidated. Moreover LMP-3 in particular is able to induce the expression of chromatin remodelling complexes in adult mesenchymal stromal cells (unpublished observation) which have been described to be involved also in the BMP-2 related osteogenic pathway [34]. LMP3 has been shown to induce certain osteogenic factors that are supposed to act in concert to induce ostegenesis in both undifferentiated and differentiated cell types, suggesting it should be able to provide an optimal balance between osteogenic and inhibitory factors. As LMP-3 is capable to induce the expression of osteogenic molecules, most of which are secreted, it likely that the osteogenic factors are released at physiologic levels *in situ* by LMP3-engineered cells.

In conclusion, our data demonstrate that LMP-3 is a potent inducer of osteogenesis for *in vivo* applications and demonstrate the efficacy of a clinically relevant approach based on autologous transplantation of dermal fibroblasts.

Materials and Methods

Construction of Recombinant Adenoviruses

E1- and E3-deleted adenoviral vector expressing human LMP3 (Ad-hLMP3), was constructed as previously described [28]. Briefly the codon-optimized LMP3 cDNA was subcloned into pcDNA3.1 TOPO T/A cloning plasmid (Invitrogen, Carlsbad, CA). A Sal I/ Not I fragment containing hLMP3, derived from the plasmid pcDNA3.1/hLMP3 was inserted in a modified version of the shuttle vector pAdlox (GenBank U62024). The adenoviral packaging cell line CRE8 was co-transfected with the Sfi I-linearized shuttle plasmid of pAdlox/hLMP3 and Ad.Ψ5 helper virus DNA. Adenoviruses were then propagated on CRE8 cells, purified by cesium chloride density gradient centrifugation and subsequent dialyzed according to standard protocols. An E1/E3-substituted recombinant adenovirus containing the cDNA for enhanced Green Fluorescent Protein (Ad-EGFP) was used as negative control.

Isolation and culture of autologous dermal fibroblasts

Cell culture mediums, sera, antibiotics, buffers, enzymes and supplements used for cell culture were purchased from Lonza (Basel, Switzerland). Primary dermal fibroblasts cultures were established using a 0.5 cm diameter punch biopsy of shaved skin obtained from the abdomen of each mouse and rat under general anesthesia and in aseptic conditions (see following section for animal models description). The tissue was washed in sterile PBS, mashed into small fragments and left for 10 minutes in an incubator at 37° C with 5% CO_2 and 85% humidity in order to enhance their adhesion to the plastic surface. Complete culture medium (Dulbecco's modified Eagles Medium, supplemented with 10% FBS, 5% horse serum, 100 units/ml penicillin and 100 μg/ml streptomycin) was then carefully added. Tissue cultures were incubated at 37° in a humidified incubator with 5% CO_2 until confluent fibroblasts layers were obtained. Tissue fragments were then removed and cells were expanded in culture for at least six passages, plated at 5×10^4 cells/cm^2 density and grown to 80% confluence for adenoviral infection.

Adenoviral-mediated transduction

Sub-confluent dermal fibroblasts were infected with either Ad.LMP-3 or Ad.EGFP using an MOI of 100 plaque forming units (pfu) per cell. Ad.EGFP was used as a vector control for testing transduction efficiency whereas untransduced cells served as additional negative control. The efficiency of adenovirus-mediated transduction was calculated by both evaluating the number of Ad.EGFP transduced cells under fluorescence microscopy and measuring transgene expression in Ad.LMP3-transduced cells by RT-PCR and quantitative real time PCR. For animal treatments, transduced cells were harvested 24 hours after viral infection, washed twice in PBS, resuspended in sterile PBS (2×10^4 cells/μl) and adsorbed on a bone conductive composite (detailed description in other paragraph of the methods section).

RT-PCR—All reagents for molecular biology methods were purchased from Invitrogen Carlsbad, CA, unless otherwise specified. The expression of the transgenic hLMP-3 was assessed in transduced cells 24 and 48 hours after infection. For this purpose total RNA was isolated from treated and control untransduced cells using Trizol reagent following manufacturer's protocol and digested with amplification grade DNase I, in order to remove genomic DNA traces in the sample, prior to reverse transcription. The yield of RNA isolation was determined using spectrophotometry (Beckman DU800, Beckman Coulter, Inc., Fullerton, CA) and the quality and integrity of total RNA was assessed by electrophoresis on 1% agarose gel in RNase-free conditions. 1 μg of purified RNA was then reverse-transcribed using SuperScript™ First-Strand Synthesis System with oligonucleotides primers according to manufacturer's suggested procedures. Finally transgenic human LMP-3 sequence was amplified using the following sequence-specific oligonucleotides: hLMP3_F: 5′-atggatagtttcaaggtc-3′ and hLMP3_R: 5′-cagccacttgaggcgggc-3′. For comparative semi-quantitative analysis of transgene expression, the beta-actin gene was amplified in the tested samples and used as housekeeping control. PCR was carried out in 50 μl volume, containing 2 μl of cDNA, 1X Buffer, 1.5mM MgCl2, 20nM deoxy ribonucleotides triphophates, 1 μM of each primer and 1 unit of Platinum Taq. Thermo-cycling conditions were as follows: initial denaturation and activation step at 95° for 2 minutes, followed by 30 cycles of 94°-58°–72° for 30 seconds each and then a final elongation step at 72° for 7 minutes. PCR products were separated by electrophoresis on 2% agarose gel, stained with ethidium bromide and analysed at UV.

Real time PCR—Transgenic LMP3 expression was quantitatively assessed by real time PCR on RNA isolated from dermal fibroblasts after 1, 2, 4, 7 and 14 days of adenoviral-mediated transduction, using Ad.EGFP-transduced cells at the same time points as negative

controls. Three independent biological replicates for each tested time point were carried out. RNA was reverse-transcribed as above described. In order to rule out genomic DNA contamination, no-reverse controls (i.e. RT reactions carried out in absence of the reverse transcriptase enzyme) were added for each sample. Thereafter, 1 μl of a 1:10 dilution of the single stranded cDNA (corresponding to 20ng) was used for real-time PCR, performed in a reaction volume of 20 μl using the SYBR green PCR master mix (Applied Biosystem, Foster City, CA) and 1 μM of LMP-sequence specific primers. Target genes were normalized to the reference housekeeping 18S ribosomal RNA gene. The analysis was performed on an ABI Prism 7900 Sequence Detection System (Applied Biosystem, Foster City, CA). The PCR conditions were as follows: an initial incubation of 50°C for 2 min and 95°C for 10 min followed by 40 cycles of 94°C for 15 s and 60°C for 1 min. Standard curves were generated for all the assays to verify PCR efficiency. The threshold cycle (CT) which correlates inversely with the levels of target mRNA, was measured as the cycle number at which the reporter fluorescence emission exceeded a preset threshold level. The amplified transcripts were quantified using the comparative CT method as previously described [35], with the formula for relative fold change= $2^{-\Delta\Delta CT}$, where ΔΔCT= [ΔCT gene of interest (treated sample) − ΔCT 5S rRNA (treated sample)] − [ΔCT gene of interest (control sample) − ΔCT 5S rRNA (control sample)]. ΔCT represents the mean CT value of each sample.

In vitro mineralization assay—Sub-confluent dermal fibroblasts plated in 6-well plates were infected with either Ad.LMP-3 or Ad.EGFP using an MOI of 100 pfu/cell. Culture medium was changed 48 hours after infection and cells were then incubated at 37° in a humidified incubator with 5% CO_2 for 14 days. Mineralization was assessed by means of Alizarin Red staining after 1 and 2 weeks post-transduction. For this purpose cells were fixed at the specified time points in 10% neutral buffered formalin and stained with Alizarin Red in order to assess the presence of calcium deposits. The experiment was performed three times in order to demonstrate reproducibility.

HA/COL nanocomposite preparation—The scaffold was assembled trough a biomimetic synthesis based on the direct nucleation of hydroxyapatite (HA) into reconstituted collagen fibers during their assembling, as already described.[36] Briefly the a phosphoric acid solution mixed with a Collagen suspension (1%) was added slowly to a $Ca(OH)_2$ aqueous solution. The cross-linking agent 1,4 butadienil diglicidil ether BDDGE was then added to act as a cross linking agent, stabilizing the polymer and reducing its solubility rate. The pH during the crystallization process was mantained in the range 10-11 and the temperature was kept around 25°C. The composites were air-dried and then freeze-dried, controlling the rate of the ice front propagation. The weight ratio of the HA/Col composite was 80:20 between HA and collagen. Total porosity was 85% with a mean macropore size ≈ 150μ and mean micropore size ≈ 5μ. The estimated crystallite size along the c axis was approximately 12 15 nm. Compounds formed in this manner conform perfectly to natural bone tissue having a mineral phase with needle-shaped morphology, nanometric dimensions, and orientation of crystallites.

Animal models and surgical procedures—Three different *ex vivo* experimental models were used to assess the bone regenerative potential of the technique: two distinct models of ectopic bone formation in mouse and one experimental model of mandibular bone defect in rat. All procedures concerning animal use and care were conducted in accordance with the laboratory of Animal Care and Use Committee of the Catholic University of Rome. All animals were randomized into three groups, according to the received treatment. Groups were as follows: group 1) autologous dermal fibroblasts transduced with Ad-LMP3 and adsorbed on the HA/COL; group 2) untransduced autologous dermal fibroblasts adsorbed on

the HA/COL scaffold; 3)HA/COL scaffold without cells, wetted with sterile PBS (referred to as naked or unseeded scaffold in other sections of the manuscript). Moreover, for each animal model, one animal per tested time point was treated with Ad-EGFP-transduced cells adsorbed on the scaffold in order to assess the persistence of fluorescent cells over time. All surgical procedures were carried out under aseptic conditions. The animals were put into separate cages in temperature controlled rooms, with a 12-h light-dark cycle and had free access to commercial food and water. Accurate post-surgical controls were carried out for all animals by periodical monitoring of body weight, wound healing process at the surgical sites and functional recovery.

Mouse ectopic bone formation in triceps muscle—Sixty 6–8 weeks-old male C57BL/6J mice were used in this protocol, assigned to protocol groups as follows: twenty in group 1, twenty in group 2 and twenty in group 3. Mice were anesthetized with a combination of 60 mg/kg ketamine and 6 mg/kg xylazine. A 0.5×0.5 cm pouch was created in the mouse triceps bilaterally through a linear incision of skin and subcutaneous tissues. The HA/COL composite was designed to be a 10×10mm sphere on which cells suspension was adsorbed. This cell-scaffold compound was then carefully introduced into the muscle pouch. Unseeded scaffold, i.e. HA/COL nanocomposite without cells, was used for negative controls as described in the previous paragraph. Wounds were then closed by sewing with vicryl. After surgery five, ten and five animals per group were sacrificed for bone formation assessment at two weeks, one month and two months, respectively.

Mouse ectopic bone formation in the paravertebral muscle—Six 6–8 weeks-old male mice C57BL/6J mice were assigned to each of the three experimental groups to be employed in this protocol. Mice were anesthetized as above indicated. The dorsal tract of the spine was reached using a posterior spine surgery approach. For this purpose a 1cm linear incision across the spinous processes was performed to expose the lamina bilaterally. In this case the HA/COL composite was modelled to form a 1cm long cylinder, which was wetted with the cell suspension or PBS alone. The scaffold was introduced along the paravertebral muscles across the exposed spine tract bilaterally. All tissues in the incision were then closed using vycril. Three mice per group were sacrificed two and four weeks, respectively, after surgery for detecting bone formation.

Rat mandibular defect—Thirty-six Wistar rats (250–300 g, Charlie-River, Italy) were used for this surgical procedure using 12 animals for each experimental group. Rats were anesthetized with an intramuscular injection of a standard anesthetic cocktail consisting of ketamine hydrochloride (50 mg/kg) and xylazine (6 mg/kg). A linear incision was made along the inferior border of the mandible, trough skin, subcutaneous tissues and masseter muscle, then the medial and lateral surfaces of the horizontal arch of the mandible were exposed using an elevator. A 5×5 mm full-thickness defect was created in the exposed mandible behind the root of the incisor using a high speed drill with irrigation, without interrupting the bone continuity. The resulting defect was filled with the cells-scaffold compound prepared as previously described. The incisions were finally closed using vicryl to sew muscle and covering skin. Four animals per group were sacrificed 4, 8 and 12 weeks after surgical procedures by lethal injection of pentobarbital sodium 150 mg/kg intraperitoneally in order to detect the bone regeneration at the osteotomised sites.

MicroCT and 3D microCT—The microCT analysis was performed using a Skyscan 1072 (Skyscan, Kontich, Belgium) consisting of a microfocus X-ray source, a rotable specimen holder and a detector system with a 1024 x 1024 pixel size CCD camera. The scanning geometry was of the cone beam type.[37,38] The X-ray projections were obtained as 12-bit grey level images and stored in 16 bit file format. The microCT used scan settings were 100

kVp, 98 μA, using 1 mm Al filter for beam hardening minimization, with 5,95 seconds exposure time and 0,45° rotation step. The magnification was set at 15 X, with a pixel size of 19 μm and with 20 × 20 mm^2 view field. The system was supplied with a 3,2 GHz Intel dual processor computer (1 Gbyte RAM). The cross-section reconstruction was performed using the CONE BEAM Reconstruction ver.2.23 software (Skyscan) and the reconstructed tomographic images were stored in 8 bit format (256 grey levels). The greylevel images have been segmented for the calculation of the bidimensional histomorphometric parameters which served for the surface area calculation, using the CT Analyser software. A global threshold was used for the segmentation of the reconstructed images (software 3D CREATOR, version 2,4 – Skyscan).

For the micro-tomographic imaging, significant portion of the treated animal were dissected. In particular, all-length spine surrounded by the paravertebral muscles bilaterally was dissected and isolated for the mouse model of ectopic bone formation in the paravertebral muscle. For rats subjected to mandible treatment the rat skull was isolated preserving muscles and soft tissues. For the CT scanning and measurements, the fresh tissues were located in an airtight cylindrical sample holder filled with formaldehyde to fix and preserve the sample for the duration of the measurement. The sample holders were marked outside with an axial line in order to obtain a consistent positioning of the specimens within the holder and to place them in the correct alignement on the microCT turntable. For all samples a total of # micro-tomographic slices with a slice increment of # μm were acquired covering the total length of the sample. The following significant morphometric indexes were calculated for both the new formed mass and the vertebral bone in the paravertebral ectopic bone model, using the Skyscan implemented software: Tissue Volume (TV, mm3) = the total volume of interest in examination, represented by the sum of all voxels in a stack of slices (corresponding to the whole new formed mass and to a section of bone of the vertebral body, respectively); Bone Volume (BV, mm3)= the sum of all voxels marked as bone inside the volume of interest; Bone Volume Fraction (BV/TV, %)= the ratio between BV and TV multiplied by 100 to have a percentage value; Bone Thickness (BT, mm)= mean thickness of bone trabeculae within the bone volume, derived from bone volume and bone surface density; Degree of Anisotropy (DA)= this value corresponds to the preferential orientation(s) of trabeculae within the bone tissue [29]. The new formed bone consisted mainly of cortical bone therefore the DA calculation was possible only for restricted area of the analyzed volume.

Histology and morphological examination—Tissue specimens were dissected, embedded in Tissue-Tek O.C.T. Compound (Bayer Healthcare, Strawberry Hill, Newbury, UK) and frozen in liquid nitrogen. 8 μm thick frozen sections were cut using a cryostate. Slides were fixed in 1% glutaraldehyde and stained using haematoxylin-eosin, Von Kossa and Alizarin methods following standard protocols in order to assess calcium deposits, matrix mineralization and osteoid formation. Moreover, tissue sections obtained from animals treated with scaffold seeded with EGFP-positive cells were analysed at fluorescence microscopy prior to the staining protocols, in order to assess the persistence of fluorescent cells and evaluate their effective adhesion and colonization of the scaffold.

Supplementary Material

Refer to Web version on PubMed Central for supplementary material.

Acknowledgments

Enrico Pola was supported by a grant of the Italian Society of Orthopaedics and Traumatology. Thanks to Kaori Okada and Sun Huijie (Department of Surgery, University of Pittsburgh School of Medicine), Filomena Pirozzi and

Alessandro Sbriccoli (Institute of Anatomy and Cell Biology, Università Cattolica del Sacro Cuore, Rome, Italy) for their precious technical assistance.

References

1. Baltzer AW, Lattermann C, Whalen JD, Ghivizzani S, Wooley P, Krauspe R, et al. Potential role of direct adenoviral gene transfer in enhancing fracture repair. Clin Orthop Relat Res. 2000; 379 (Suppl):S120–5. [PubMed: 11039760]
2. Lattanzi W, Pola E, Pecorini G, Logroscino CA, Robbins PD. Gene therapy for in vivo bone formation: recent advances. Eur Rev Med Pharmacol Sci. 2005; 9(3):167–74. [PubMed: 16080636]
3. Blum JS, Barry MA, Mikos AG, Jansen JA. In vivo evaluation of gene therapy vectors in ex vivo-derived marrow stromal cells for bone regeneration in a rat critical-size calvarial defect model. Hum Gene Ther. 2003; 14(18):1689–701. [PubMed: 14670121]
4. Chang SC, Chuang HL, Chen YR, Chen JK, Chung HY, Lu YL, et al. Ex vivo gene therapy in autologous bone marrow stromal stem cells for tissue-engineered maxillofacial bone regeneration. Gene Ther. 2003; 10(24):2013–9. [PubMed: 14566360]
5. Lee JY, Peng H, Usas A, Musgrave D, Cummins J, Pelinkovic D, et al. Enhancement of bone healing based on ex vivo gene therapy using human muscle-derived cells expressing bone morphogenetic protein 2. Hum Gene Ther. 2002; 13 (10):1201–11. [PubMed: 12133273]
6. Lieberman JR, Daluiski A, Stevenson S, Wu L, McAllister P, Lee YP, et al. The effect of regional gene therapy with bone morphogenetic protein-2-producing bone-marrow cells on the repair of segmental femoral defects in rats. J Bone Joint Surg Am. 1999; 81(7):905–17. [PubMed: 10428121]
7. Mauney JR, Kaplan DL, Volloch V. Matrix-mediated retention of osteogenic differentiation potential by human adult bone marrow stromal cells during ex vivo expansion. Biomaterials. 2004; 25(16):3233–43. [PubMed: 14980418]
8. Mauney JR, Jaquiery C, Volloch V, Heberer M, Martin I, Kaplan DL. In vitro and in vivo evaluation of differentially demineralized cancellous bone scaffolds combined with human bone marrow stromal cells for tissue engineering. Biomaterials. 2005; 26(16):3173–85. [PubMed: 15603812]
9. Moutsatsos IK, Turgeman G, Zhou S, Kurkalli BG, Pelled G, Tzur L, et al. Exogenously regulated stem cell-mediated gene therapy for bone regeneration. Mol Ther. 2001; 3(4):449–61. [PubMed: 11319905]
10. Peng H, Wright V, Usas A, Gearhart B, Shen HC, Cummins J, et al. Synergistic enhancement of bone formation and healing by stem cell-expressed VEGF and bone morphogenetic protein-4. J Clin Invest. 2002; 110(6):751–9. [PubMed: 12235106]
11. Sugiyama O, An DS, Kung SP, Feeley BT, Gamradt S, Liu NQ, et al. Lentivirus-mediated gene transfer induces long-term transgene expression of BMP-2 in vitro and new bone formation in vivo. Mol Ther. 2005; 11(3):390–8. [PubMed: 15727935]
12. Tsuda H, Wada T, Yamashita T, Hamada H. Enhanced osteoinduction by mesenchymal stem cells transfected with a fiber-mutant adenoviral BMP2 gene. J Gene Med. 2005; 7(10):1322–34. [PubMed: 15926193]
13. Yang M, Ma QJ, Dang GT, Ma K, Chen P, Zhou CY. In vitro and in vivo induction of bone formation based on ex vivo gene therapy using rat adipose-derived adult stem cells expressing BMP-7. Cytotherapy. 2005; 7(3):273–81. [PubMed: 16081354]
14. Wang JC, Kanim LE, Yoo S, Campbell PA, Berk AJ, Lieberman JR. Effect of regional gene therapy with bone morphogenetic protein-2-producing bone marrow cells on spinal fusion in rats. J Bone Joint Surg Am. 2003; 85:905–11. [PubMed: 12728043]
15. Zhang XS, Linkhart TA, Chen ST, Peng H, Wergedal JE, Guttierez GG, et al. Local ex vivo gene therapy with bone marrow stromal cells expressing human BMP4 promotes endosteal bone formation in mice. J Gene Med. 2004; 6(1):4–15. [PubMed: 14716672]
16. Nussenbaum B, Rutherford RB, Teknos TN, Dornfeld KJ, Krebsbach PH. Ex vivo gene therapy for skeletal regeneration in cranial defects compromised by postoperative radiotherapy. Hum Gene Ther. 2003; 14(11):1107–15. [PubMed: 12885349]

17. Shen HC, Peng H, Usas A, Gearhart B, Cummins J, Fu FH, Huard J. Ex vivo gene therapy-induced endochondral bone formation: comparison of muscle-derived stem cells and different subpopulations of primary muscle-derived cells. Bone. 2004; 34 (6):982–92. [PubMed: 15193544]
18. Rutherford RB, Moalli M, Franceschi RT, Wang D, Gu K, Krebsbach PH. Bone morphogenetic protein-transduced human fibroblasts convert to osteoblasts and form bone in vivo. Tissue Eng. 2002; 8(3):441–52. [PubMed: 12167230]
19. Gugala Z, Olmsted-Davis EA, Gannon FH, Lindsey RW, Davis AR. Osteoinduction by ex vivo adenovirus-mediated BMP2 delivery is independent of cell type. Gene Ther. 2003; 10(16):1289–96. [PubMed: 12883525]
20. Hirata K, Tsukazaki T, Kadowaki A, Furukawa K, Shibata Y, Moriishi T, et al. Transplantation of skin fibroblasts expressing BMP-2 promotes bone repair more effectively than those expressing Runx2. Bone. 2003; 32(5):502–12. [PubMed: 12753866]
21. Krebsbach PH, Gu K, Franceschi RT, Rutherford RB. Gene therapy-directed osteogenesis: BMP-7-transduced human fibroblasts form bone in vivo. Hum Gene Ther. 2000; 11(8):1201–10. [PubMed: 10834621]
22. Nakashima K, Zhou X, Kunkel G, Zhang Z, Deng JM, Behringer RR, et al. The novel zinc finger-containing transcription factor osterix is required for osteoblast differentiation and bone formation. Cell. 2002; 108(1):17–29. [PubMed: 11792318]
23. Viggeswarapu M, Boden SD, Liu Y, Hair GA, Louis-Ugbo J, Murakami H, et al. Adenoviral delivery of LIM mineralization protein-1 induces new-bone formation in vitro and in vivo. J Bone Joint Surg Am. 2001; 83-A(3):364–76. [PubMed: 11263640]
24. Boden SD, Liu Y, Hair GA, Helms JA, Hu D, Racine M, et al. LMP-1, a LIM-domain protein, mediates BMP-6 effects on bone formation. Endocrinology. 1998; 139(12):5125–34. [PubMed: 9832452]
25. Boden SD, Titus L, Hair G, Liu Y, Viggeswarapu M, Nanes MS, et al. Lumbar spine fusion by local gene therapy with a cDNA encoding a novel osteoinductive protein (LMP-1). Spine. 1998; 23(23):2486–92. [PubMed: 9854747]
26. Liu Y, Hair GA, Boden SD, Viggeswarapu M, Titus L. Overexpressed LIM mineralization proteins do not require LIM domains to induce bone. J Bone Miner Res;. 2002; 17(3):406–14.
27. Sangadala S, Boden SD, Viggeswarapu M, Liu Y, Titus L. LIM mineralization protein-1 potentiates bone morphogenetic protein responsiveness via a novel interaction with Smurf1 resulting in decreased ubiquitination of Smads. J Biol Chem. 2006; 281(25):17212–9. [PubMed: 16611643]
28. Pola E, Gao W, Zhou Y, Pola R, Lattanzi W, Sfeir C, et al. Efficient bone formation by gene transfer of human LIM mineralization protein-3. Gene Ther. 2004; 11 (8):683–93. [PubMed: 14724674]
29. Müller R, Van Campenhout H, Van Damme B, Van Der Perre G, Dequeker J, Hildebrand T, Rüegsegger P. Morphometric analysis of human bone biopsies: a quantitative structural comparison of histological sections and micro-computed tomography. Bone. 1998; 23(1):59–66. [PubMed: 9662131]
30. Wernig M, Meissner A, Foreman R, Brambrink T, Ku M, Hochedlinger K, Bernstein BE, Jaenisch R. *In vitro* reprogramming of fibroblasts into a pluripotent ES-cell-like state. Nature. 2007; 448(7151):318–24. [PubMed: 17554336]
31. Landi E, Logroscino G, Proietti L, Tampieri A, Sandri M, Sprio S. Biomimetic Mg-substituted hydroxyapatite: from synthesis to in vivo behaviour. J Mater Sci Mater MedJ Mater Sci Mater Med. 2008; 19(1):239–47.
32. Minamide A, Boden SD, Viggeswarapu M, Hair GA, Oliver C, Titus L. Mechanism of bone formation with gene transfer of the cDNA encoding for the intracellular protein LMP-1. J Bone Joint Surg Am. 2003; 85-A(6):1030–9. [PubMed: 12783998]
33. Yoon ST, Park JS, Kim KS, Li J, Attallah-Wasif ES, Hutton WC, Boden SD. ISSLS prize winner: LMP-1 upregulates intervertebral disc cell production of proteoglycans and BMPs in vitro and in vivo. Spine. 2004; 29(23):2603–11. [PubMed: 15564908]
34. Young DW, Pratap J, Javed A, Weiner B, Ohkawa Y, van Wijnen A, Montecino M, Stein GS, Stein JL, Imbalzano AN, Lian JB. SWI/SNF chromatin remodeling complex is obligatory for

BMP2-induced, Runx2-dependent skeletal gene expression that controls osteoblast differentiation. J Cell Biochem. 2005; 94(4):720–30. [PubMed: 15565649]

35. Livak KJ, Schmittgen TD. Analysis of relative gene expression data using real-time quantitative PCR and the 2(−Delta Delta C(T)) Method. Methods. 2001; 25(4):402–8. [PubMed: 11846609]
36. Tampieri A, Celotti G, Landi E, Sandri M, Roveri N, Falini G. Biologically inspired synthesis of bone-like composite: self-assembled collagen fibers/hydroxyapatite nanocrystals. J Biomed Mater Res A. 2003; 67(2):618–25. [PubMed: 14566805]
37. Feldkamp LA, Goldstein SA, Parfitt AM, Jesion G, Kleerekoper M. The direct examination of three-dimensional bone architecture in-vitro by computed tomography. J Bone Miner Res. 1989; 4:3–11. [PubMed: 2718776]
38. Sasov AY. Microtomography. Part 1: Methods and equipment. J Microsc. 1987; 147:169–78.

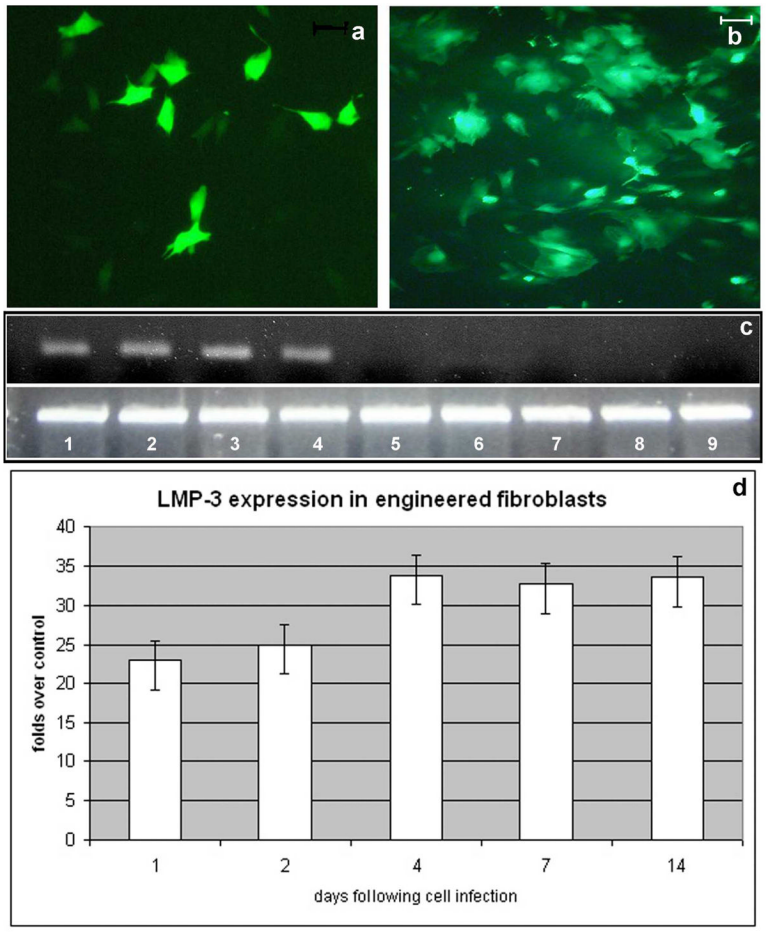

Figure 1. Efficiency of adenoviral-mediated transduction of dermal fibroblasts

Dermal fibroblast isolated in primary culture from skin biopsies were infected using a defective adenoviral vector carrying either the LMP-3 or the EGFP gene: EGFP served as a reporter gene which allowed to assess the transgene expression *in vitro* by counting EGFP-positive cells under fluorescent invertoscope at 24 hours **(a)** and 48 hours **(b)** after transduction; scale bar: 10μm; **c)** transgene expression in Ad.LMP-3 transduced cells was assessed at the same time points by means of RT-PCR using sequence-specific primers for the human LMP3 gene (upper gel row) and the housekeeping beta-actin gene as a control for normalization (lower gel row): lane 1 and 2 LMP-3-transduced cells 24 hours post-infection; lane 3 and 4 AdLMP-3-transduced cells 48 hours post-infection; lane 5 and 6 AdEGFP-transduced cells 24 hours post-infection; lane 7 and 8 AdEGFP-transduced cells 24 hours post-infection; lane 9 untransduced dermal fibroblasts. **d)** LMP-3 expression was quantified in dermal fibroblasts infected with Ad.hLMP-3 by means of quantitative real-time PCR in time-course up to 14 days. Cells were harvested for mRNA isolation at specified time-points after adenoviral-mediated transduction and transgene expression was examined by real time PCR using sequence specific primers. The beta-actin gene was amplified by real time PCR from the same RNA samples and used as a housekeeping control gene. Expression levels are expressed as fold change over the control, which was calculated according to the ΔΔCt method as reported in the methods section.

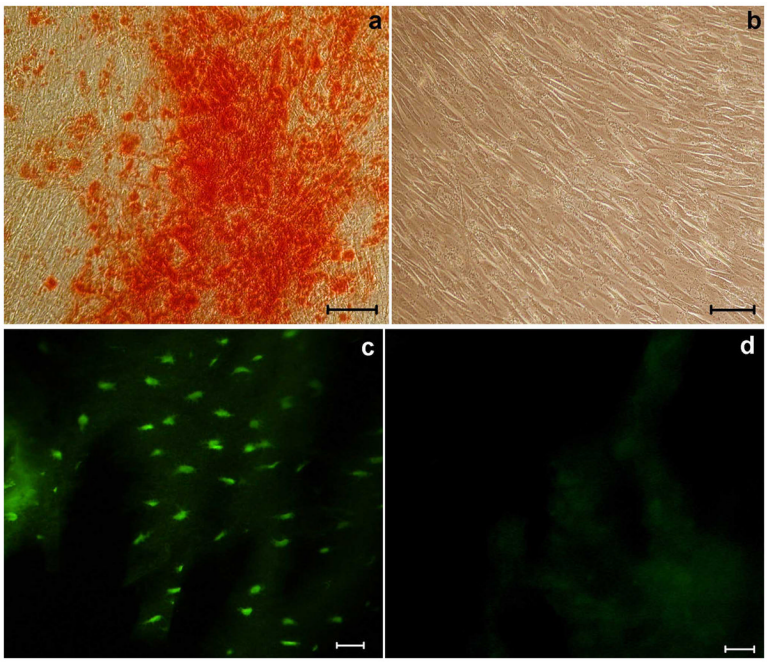

Figure 2. Intrinsic osteogenic potential *in vitro* of engineered dermal fibroblasts and persistence of transgene expression *in vivo*

Red alizarin staining was performed one week after cell infection aimed at evaluating the osteogenic potential *in vitro* of LMP3-transduced dermal fibroblasts. The assay showed red-coloured calcium deposits in LMP-3-transduced dermal fibroblasts (**a**), while no red-stained mineralized matrix could be demonstrated in the control EGFP-transduced cells (**b**). Fluorescence microscopy was used to assess wether transgene expression persisted *in vivo* over time after the implantation in fresh tissue sections: **c.** rat mandibula treated with EGFP-transduced fibroblasts seeded on the HA/COL scaffold, one month after surgery; **d.** rat mandibula treated with unseeded biomaterial at the same time point. Scale bar: 10 μm in all panels.

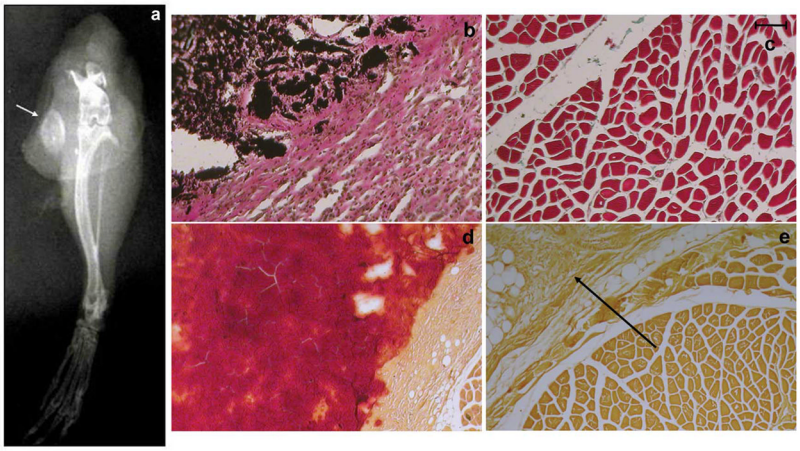

Figure 3. X-ray and histological analysis of the extent of ectopic bone formation following implantation of adenoviral transduced dermal fibroblasts in murine triceps muscles

a. X-rays obtained from mouse leg 2 months after the implantation of Ad.LMP3-transduced cells seeded on the HA/COL scaffold in triceps, the arrow points out a radiopaque mass at the site of implantation; **b**. Von Kossa staining obtained 1 month after the implantation of Ad.LMP3-transduced cells seeded on the HA/COL scaffold, the dark brown-coloured area indicates calcium deposits (i.e. mineralized tissue) at the site of implantation, bordered by reactive connective tissue with infiltrating mononuclear cells; **c**. Von Kossa staining in control muscle tissue; **d–e**. positive and negative Alizarin stainings obtained 2 months after the implantation of Ad.LMP3- and mock-transduced cells, respectively. Dark red coloured area represents the new mineralized matrix formed within the muscle. The arrow points out the non-mineralized reactive tissue infiltrating HA/COL residuals. Scale bar: 1 mm in all histological panels

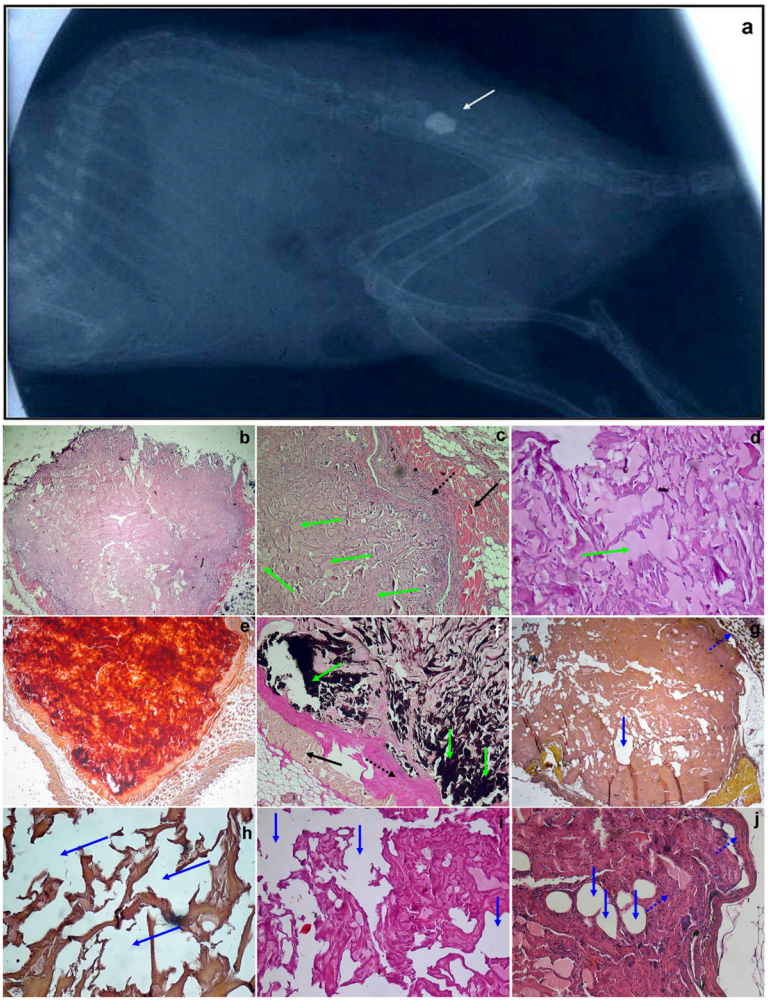

Figure 4. X-ray and histological analysis of the extent of ectopic bone formation following implantation of the HA/COL scaffold seeded with adenoviral transduced dermal fibroblasts into the mouse paravertebral muscle

a. Positive X-ray showing a radiopaque mass (arrow) at the site of implantation 2 months after the treatment. **b–f**. Histological stainings obtained 1 month after LMP3-transduced cells implantation in the paravertebral mouse muscle: haematoxylin-eosin stainings 20X (**b**), 30X (**c**) and 40X (**d**); **e.** positive alizarin staining (20X) showing red-coloured mineralized matrix within the neo-formed tissue; **f.** positive Von Kossa staining (30X). Histological stainings obtained 1 month after control cells implantation in the paravertebral mouse muscle: **g.** negative Von Kossa staining (30X) and **h.** same image at higher magnification (50X), the arrows indicate empty spots within the non-mineralized mass, suggesting the presence of reabsorbing HA/COL; **i.** haematoxylin-eosin stainings 50X and **j** same image at higher magnification. ***Green arrows*** indicate areas with bone morphology, red-coloured mineralized matrix and dark brown-coloured mineralized areas within the neo-formed tissue evidenced with haematoxylin-eosin, aliazarin and Von Kossa methods, respectively; ***dotted black* arrows** indicate fibrous tissue surrounding the new-formed mass; ***black arrows*** indicate muscle; ***blue arrows*** indicate empty spots within the non-mineralized mass, suggesting the presence of reabsorbing HA/COL, ***dotted blue arrows*** indicate fibrous tissue surrounding and infiltrating the scaffold.

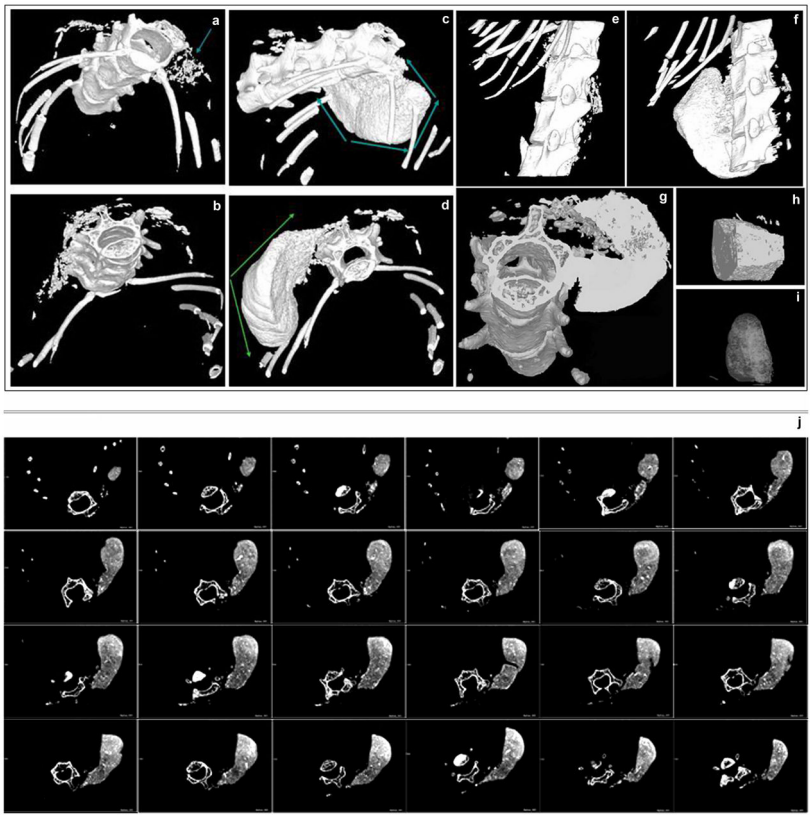

Figure 5. μCT analysis and 3D reconstruction of the extent of ectopic bone formation following implantation of the HA/COL scaffold seeded with adenoviral transduced dermal fibroblasts into the paravertebral muscle

3D MicroCT images obtained from control and LMP3-treated animals two month after surgery: no significant bone/like structures mass is detected animals treated with either untransduced cells seeded on scaffold (**a.**) or naked scaffold (**b.**), arrow indicates the site of implantation; new bone formation at the site of implantation is detected in animals treated with Ad.LMP-3 modified autologous fibroblasts 2 months after surgery (**c** and **d**), arrows display the CT dense mass at the site of implantation. The results are confirmed in a 3D lateral view reconstruction: **e.** mouse treated with the unseeded scaffold, **f.** dense mass in the LMP3-treated animal. The new formed bone exhibits the same density of the cortical bone in axial view (**g**) and in 3D reconstruction of two sections of the new formed bone obtained from different animals (**h** and **i**). The lower panels (**j**) display serial cross axial sections of a LMP-3 treated mouse showing spots of cortical bone-like density within the new formed mass flanking the spine. See table 2 for morphometric indexes calculated on the newly formed mass in treated animals.

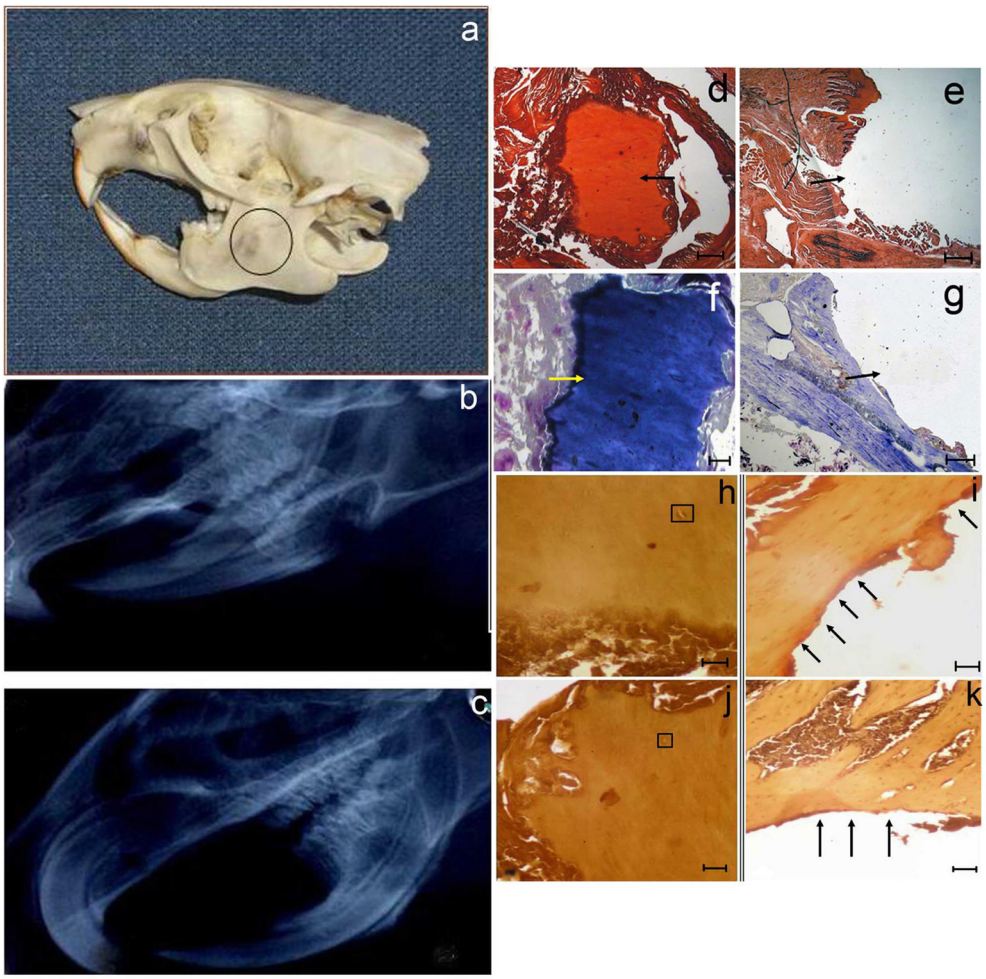

Figure 6. X-ray and histological analysis of the extent of bone formation following the implantation of the HA/COL scaffold seeded with adenoviral transduced dermal fibroblasts into the mandibular bone defect

a. Skull model of the mandibular bone defect: a circular defect, with a diameter of about 0.5 cm, was created posteriorly to the root of the incisor. The resulting defect was filled with the unseeded scaffold or with the scaffold seeded with adenoviral transduced autologous dermal fibroblasts. No bone formation is observed in rats receiving unseeded biomaterial (**b**) while the defect is partially filled with new formed radio-opaque tissue as shown by X-ray analysis, indicating local bone formation at the site of implantation, in a rat treated with LMP3-expressing cells 3 months after surgery (**c**). Histological examination shows the surgical hole filled with new bone four months after LMP3 treatment: **d** and **e**) positive and negative Alizarin stainings; **f** and **g**) positive and negative Toluidin Blue staining (arrows indicate the defect area); ***arrows*** indicate the defect area filled with a mineralized matrix and the empty surgical hole, in treated and control animals, respectively; **h–k**) section coloured with haematoxylin-eosin methods showing bone morphology in the newly formed tissue at the site of implantation of LMP3-transduced fibroblasts adsorbed on the HA/COL (**h** and **j**) and empty defect area in animal treated with naked scaffold (**i** and **k**). ***Arrows*** indicate the tissue bordering the perimeter of the surgical hole; ***squares*** enclose haversian canals in the new-formed compact bone. Different stainings are from different animals enrolled in the protocol. Negative staining confirm that the bone defect was not healed up to four months

after implantation of the scaffold with control cells (**e** and **g**) and unseeded scaffold (**i** and **k**). Scale bars: 1mm in panels d, e, g, I and k; 0,5 mm in panel f; 0,1mm in panels h and j.

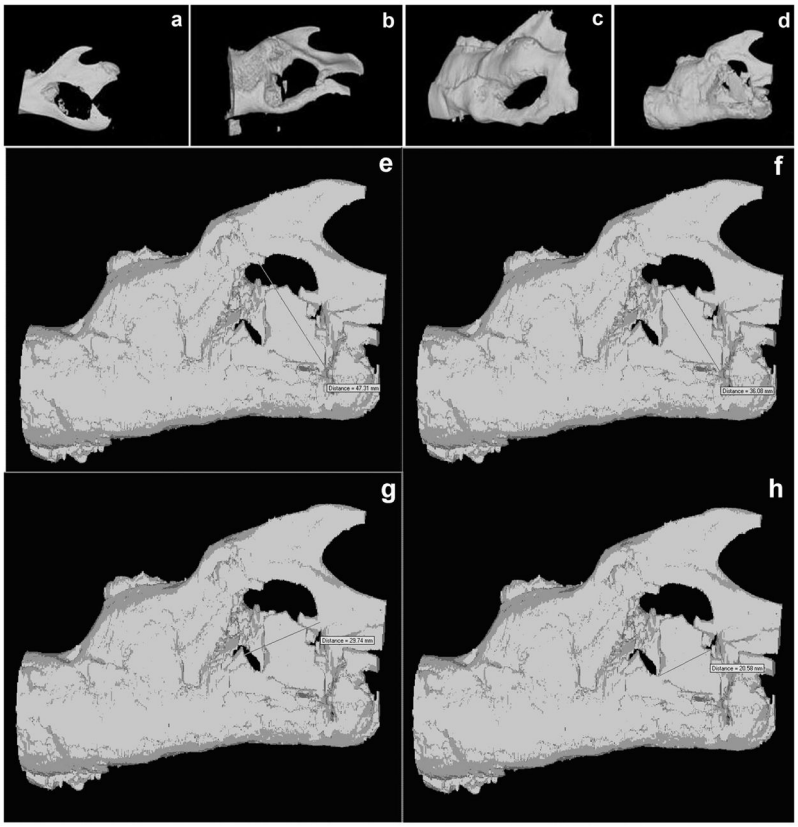

Figure 7. 3DμCT analysis of the mandibular bone defect healing following the treatment

3D reconstruction of μCT scan images were obtained from rat mandibles after sacrifice: **a.** control mandible treated with unseeded scaffold at 8 weeks after surgery, **b.** mandible treated with LMP3-transduced cells seeded on the HA/COL after 4 weeks, **c.** after 8 weeks and **d.** after 12 weeks: the bone gap is partially filled with a CT dense tissue indicating local bone formation in rats 12 weeks after receiving the LMP3 treatment. Lower panels show the empirical calculation methods of the surface areas: **e** and **f.** major diameters of the whole defect area and of the new formed dense mass, respectively; **g** and **h**. minor diameters of the whole defect area and of the new formed dense mass, respectively; the four images are all from the same animal. Surface areas were calculated in each animal based on the mean diameter measure and compared to the surface area of the defect in order to obtain a defect-filling ratio.

Table 1

summary of results in the three experimental models

Triceps ectopic bone formation (mouse)			
Time point	**Number of treated animals**	**Number of positive mice by X-rays and histology**	**Number of negative mice by X-rays and histology**
2 weeks	5	1	4
4 weeks	10	6	4
8 weeks	5	3	2
total	20	10	10

Paravertebral ectopic bone formation (mouse)			
Time point	**Number of treated animals**	**Number of positive mice by X-rays, μCT and histology**	**Number of negative mice by X-rays, μCT and histology**
4 weeks	3	3	0
8 weeks	3	3	0
total	6	6	0

Mandibular bone defect (rat)			
Time point	**Number of treated animals**	**Number of positive rats by X-rays, μCT and histology**	**Number of positive rats by X-rays, μCT and Histology**
4 weeks	4	1	3
8 weeks	4	4	0
12 weeks	4	4	0
total	12	9	3

[a]Number of positive radiological imaging (X-rays or CT) and histology assays obtained for animals subjected to LMP3-transduced cells implantation sacrificed at the specified time points in the three experimental models.

Table 2

μCT morphometric indexes: comparative analysis of the new formed bone and vertebral bone structure

	New formed mass[a]	Vertebral bone[b]
TV (mm^3)	83,910 ± 20.056[c]	1,990 ± 0,976
BV (mm^3)	25,348 ± 10.102	0,890 ± 0,333
BV/TV (%)	30,200 ± 2.121	46,293 ± 4,650
BT (mm)	0,134 ± 0.057	0,117 ± 0.012
DA	1,414 ± 0.102	1,377 ± 0.021

[a] Indexes were calculated on the CT dense tissue formed *ex novo* in mice treated with LMP3-transduced autologous dermal fibroblasts on the HA/COL, one month after surgery;

[b] corresponding measures calculated in small sections (comprised of both cortical and trabecular bone) of the vertebral body of the same mice;

[c] values have been calculated as mean ± standard deviation of allbiological replicates in the treatment group. All acronimes used in the table are explained in text (see methods section).